FOI-R–0550–SE
December 2002
ISSN 1650-1942

Methodology report

Mattias Unosson

Shock wave loading of concrete grout using a plane wave generator

Weapons and protection division
SE-147 25 TUMBA

FOI – Swedish Defence Research Agency
Weapons and protection division
SE-147 25 TUMBA

FOI-R–0550–SE
December 2002
ISSN 1650-1942

Methodology report

Mattias Unosson

Shock wave loading of concrete grout using a plane wave generator

Weapons and protection division
SE-147 25 TUMBA

Abstract

In the report a series of experiments is presented where solid discs of concrete grout are loaded with plane shock waves. Plane wave generators with high explosives were used for the loading, and registration of stress and times of arrival were made using calibrated piezoelectric stress gauges (PVDF) and piezoelectric pins. Finite element analysis was used to design the experimental set-up. From the experimental results, points on the equation of state for the grout were derived through impedance matching with Lexan. The amplitudes from the gauges, representing the pressure level, were too low due to shortage of the gauges. The grout specimens had been kept in water prior to the experiments to minimize the risk of cracks. The conclusions were that the experimental technique used is suitable for deriving points on the equation of state at pressure levels above $15\ GPa$.

Contents

List of Figures

List of Tables

1 Introduction

1.1 Background

It is impossible to experimentally characterize the mechanical behaviour of materials for all deformation paths, since there are an infinite number of possibilities. In solid mechanics we instead characterize the material for a finite number of loading paths and use the result as basis for a mathematical model. For a constitutive equation to be valid for an arbitrary loading, additional information is needed.

Continuum mechanics is the mechanics for deformable media without consideration of its internal structure. However, with knowledge of the material's internal structure it is possible to obtain information on material symmetry. Additional information is extracted through interpolation and extrapolation of the experimental data at hand. Extrapolation should be minimized by ensuring that the experimental data spans the solution space for the problem studied. Further, discrete input data representing continuous functions should be sufficiently many in numbers in order to minimize interpolation.

When modelling porous materials such as *concrete grout* the material behaviour is split into a deviatoric and a volumetric part where an *equation of state (EOS)* governs the latter. This is due to the simplification that this imposes on the material description. The equation of state can be interpreted as a surface in the (ρ, p, e)-space where ρ is the mass density, p is the volumetric pressure and e is the internal energy. Focusing on the equation of state and problems involving *conventional weapons loading* the input must cover the range of volumetric pressures that occur in the model. Typical maximum levels of compressive pressures in a concrete target impacted by a projectile at ordnance velocity are of order $10^9\ Pa$ and strain rates of order $10^4\ s^{-1}$.

Today methods exists for producing quasi-static, compressive pressure loading up to $10\,GPa$ from which isothermal compaction curves are extracted. But, this curve represents only a meridian, orthogonal with respect to the internal energy, on the equation of state surface. For dynamic loading and higher pressures, i.e. for more points on the EOS-surface, other techniques have to be used. One could apply the quasi-static load at different temperatures, but there are a number of experimental techniques available for dynamic loading of solid material that involve shock waves, such as:

- Plane wave high explosive generators
- Projectile impact (Plate-impact etc.)
- Others (Pulsed lasers, nuclear devices etc.)

See Meyers [1] or Graham [2] for an overview of such methods. In this work *plane wave generators* have been used due to low investment costs and short start-up time.

Shock waves are defined as singular surfaces of first order causing a jump in the velocity deformation gradient fields and consequently in the strain and stress fields, cf. Truesdell and Toupin [3]. Shock waves in solids are commonly divided into one of the three following categories:

- Elastic shock (within the elastic domain travelling at the elastic shock velocity)

- Elastic-inelastic shock (into the inelastic domain where the shock velocity is below the elastic one, causing an elastic precursor wave in some materials)
- Strong shock (into the inelastic domain where the shock velocity exceeds the elastic one)

Depending on the mechanical properties of a material, a shock wave can transform from one type to another when travelling through a solid. In this work strong planar shock waves are considered, in which the material is subjected to loading in *uniaxial deformation* up to a peak pressure and followed by isentropic unloading, i.e. without any heat flow. The uniaxial state of deformation, and neglecting material deviatoric strength, renders a simple theory for analysis of the shock waves, the so called Rankine-Hugoniot field equations, c.f. for example Meyers [1]. The shock loading process is monitored using so called diagnostic tools that are, based on their physical properties, divided into:

- Piezoelectric (generates an electrical charge upon loading)
- Piezoresistive (changes its electrical resistance upon loading)
- Electromagnetic
- Optical

In this work two types of piezoelectric tools have been used, *piezoelectric pins* and *polyvinylidene difluoride (PVDF) gauges*, c.f. Meyers [1] or Graham [2].

1.2 Purpose

Analyses of protective structures with a well set-up finite element model can reduce the number of experiments, and thus costs for the customer. The input parameters from mechanical material characterization must match the material states to occur in the model, i.e. characterization methods involving dynamic loading must be used. The purpose of this work was to assess the potential of plane wave generators as in-house method to characterize concrete grout.

2 Method

2.1 Numerical analysis

Numerical analysis was performed to design the experimental set-up. For this Autodyn [4] double precision version 4.2.03a was used in a Windows 2000 environment operating on double 2 GHz Pentium Xeon processors with 2 GB main memory. Autodyn uses finite difference schemes to solve the equations of continuum mechanics, c.f. Truesdell and Noll [5]. Two-dimensional models with rotational symmetry were used, and the number of elements varied between 216500 and 405200.

2.1.1 Kinematics

Spatial description of the motion, i.e. Eulerian formulation, was used for all computations.

2.1.2 Dynamics

All parameters used for the constitutive equations are found in Appendix A.

High explosives

The high explosive, TNT, was modelled with the JWL equation of state, cf. Lee et al. [6] or the Autodyn theory manual [4]. The parameters were taken from the Autodyn material library.

Lexan

Lexan (polycarbonate) was used as a reference and damping material since its shoch wave properties are well known. This material was modelled in the deviatoric domain as an isotropic linear-elastic, perfectly plastic material with a von Mises yield condition. The volumetric behaviour was modelled with the Mie-Grüneisen shock EOS, cf. [1]. A linear equation of state was fitted to experimental data from Marsh [7] in the expected shock-velocity domain.

Concrete grout

The concrete grout, with aggregates $\leq 1\,mm$, was modelled with the $p-\alpha$ EOS, c.f. Riedel [8], and elastic-perfect plasticity with the von Mises yield criterion. The parameters were taken from Wicklein [9], a report from a previous characterization campaign performed at EMI in Germany on this particular concrete grout. The composition of the concrete grout is given in Table 1. See Smeplass [10] for a detailed description.

Steel

Finally, the steel backing plate (quality SS 14 1650) was modelled with the Johnson-Cook model, c.f. Johnson and Cook [11] and the Mie-Grüneisen shock EOS. The material parameters were taken from the Autodyn material library (valid for quality AIS 1006).

Table 1. Composition of the concrete grout

Component	**Mass** $[kg/m^3]$
Cement	1120.6
Microsilica	224.1
Free water	309.3
Absorbed water	2.1
Aggregates $(0 - 1\,mm)$	528.8
Plasticizer	56.0

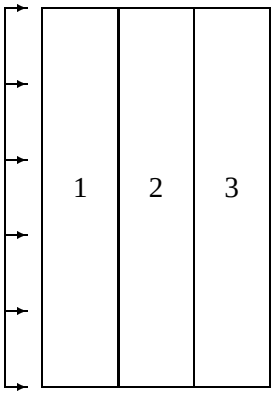

Figure 1. Shematic figure of the initial phase (phase 0) of the experiment

2.2 Plane wave experiments

2.2.1 Theory

Three materials are used in the experiments of which two with known equation of state (specimens one and three) and one unknown (specimen two), see Figure 1. Measurements are made on the specimen volumes and masses respectively giving their initial densities. A plane shock wave enters specimen 1 and propagates through all three specimens. The differences in shock wave arrival times together with specimen thicknesses yields the mean shock-wave velocities that are used to derive material properties.

Assuming the shear modulus of the material to be zero, body forces to be negligible, adiabatic heating at the shock front and the wave to be perfectly plane, we can use the following jump conditions, c.f. Meyers [1]:

$$\rho\,(u - v) = \rho_0\,(u - v_0) \tag{1}$$

$$p - p_0 = \rho_0\,(u - v_0)\,(v - v_0) \tag{2}$$

$$e - e_0 = \frac{1}{2}\,(p + p_0)\left(\frac{1}{\rho_0} - \frac{1}{\rho}\right) \tag{3}$$

Here u is the shock front velocity, v is the corresponding particle velocity, ρ is the density, p is the hydrostatic pressure and e is the internal energy and index 0 denotes state variables in front of the shock wave.

The equation of state, ie. the constitutive equation, is formulated on Grüneisen form with a linear $u - v$-relation as reference state according to

$$p = p_H + \rho g_j\,(e - e_H) \tag{4}$$

$$u = c_j + s_j v \tag{5}$$

where g_j, c_j and s_j are material parameters. A linear $u - v$-relation does not encompass elastoplastic behaviour, phase transformations nor porosity in the material. These equations together with the conditions of equilibrium and continuity across material boundaries, that there is no release nor attenuation of the shock wave form the basis for extracting data from the experiments. Here follows a description of each phase of the process and the change in its state variables. All secondary reflections, refractions and interactions are ignored and the variables are indexed i, j which denotes the state and specimen respectively.

Phase 0

In the initial phase the shock wave has not yet reached specimen one and all specimens are still in their initial state with known state variables.

$$\left.\begin{aligned} \rho_{0,1} &= \rho_{0,1}^{exp.} \\ p_{0,1} &= 0 \\ e_{0,1} &= 0 \end{aligned}\right\} \tag{6}$$

$$\left.\begin{aligned} \rho_{0,2} &= \rho_{0,2}^{exp.} \\ p_{0,2} &= 0 \\ e_{0,2} &= 0 \end{aligned}\right\} \tag{7}$$

$$\left.\begin{aligned} \rho_{0,3} &= \rho_{0,3}^{exp.} \\ p_{0,3} &= 0 \\ e_{0,3} &= 0 \end{aligned}\right\} \tag{8}$$

Phase 1

In phase one the shock wave front propagates through specimen one according to

$$\left.\begin{aligned} \rho_{1,1}\left(u_{1,1} - v_{1,1}\right) &= \rho_{0,1}u_{1,1} \\ p_{1,1} &= \rho_{0,1}u_{1,1}v_{1,1} \\ e_{1,1} &= \tfrac{1}{2}p_{1,1}\left(\tfrac{1}{\rho_{0,1}} - \tfrac{1}{\rho_{1,1}}\right) \\ u_{1,1} &= c_1 + s_1 v_{1,1} \end{aligned}\right\} \tag{9}$$

$$\left.\begin{aligned} \rho_{1,2} &= \rho_{0,1}^{exp.} \\ p_{1,2} &= 0 \\ e_{1,2} &= 0 \end{aligned}\right\} \tag{10}$$

$$\left.\begin{aligned} \rho_{1,3} &= \rho_{0,3}^{exp.} \\ p_{1,3} &= 0 \\ e_{1,3} &= 0 \end{aligned}\right\} \tag{11}$$

Inserting experimental results and solving for unknown parameters results in

$$\left.\begin{aligned} v_{1,1} &= \tfrac{u_{1,1}^{exp.} - c_1}{s_1} \\ \rho_{1,1} &= \tfrac{\rho_{0,1}}{1 - \frac{1}{s_1} + \frac{c_1}{s_1 u_{1,1}^{exp.}}} \\ p_{1,1} &= \tfrac{\rho_{0,1}}{s_1}\left(u_{1,1}^{exp.} - c_1\right)u_{1,1}^{exp.} \\ e_{1,1} &= \tfrac{\left(u_{1,1}^{exp.} - c_1\right)^2}{2s_1^2} \end{aligned}\right\} \tag{12}$$

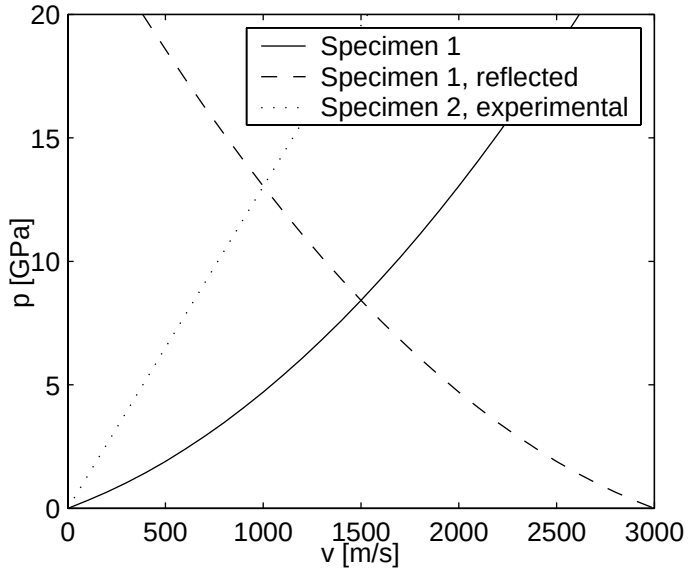

Figure 2. Impedance matching

Phase 2

In phase two the wave front has reached the material interface where it is refracted and reflected back into the pre-shocked specimen one according to

$$\left.\begin{aligned} &\rho_{2,1}\left(u_{2,1}-v_{2,1}\right)=\rho_{1,1}\left(u_{2,1}-v_{1,1}\right)\\ &p_{2,1}-p_{1,1}=\rho_{1,1}\left(u_{2,1}-v_{1,1}\right)\left(v_{2,1}-v_{1,1}\right)\\ &e_{2,1}-e_{1,1}=\tfrac{1}{2}\left(p_{2,1}+p_{1,1}\right)\left(\tfrac{1}{\rho_{1,1}}-\tfrac{1}{\rho_{2,1}}\right)\\ &p_{2,1}=p_{1,1}+\tfrac{1}{2}\left(\rho_{1,1}+\rho_{2,1}\right)g_1\left(e_{2,1}-e_{1,1}\right) \end{aligned}\right\} \tag{13}$$

$$\left.\begin{aligned} &\rho_{2,2}\left(u_{2,2}-v_{2,2}\right)=\rho_{1,2}u_{2,2}\\ &p_{2,2}=\rho_{1,2}u_{2,2}v_{2,2}\\ &e_{2,2}=\tfrac{1}{2}p_{2,2}\left(\tfrac{1}{\rho_{1,2}}-\tfrac{1}{\rho_{2,2}}\right) \end{aligned}\right\} \tag{14}$$

$$\left.\begin{aligned} &\rho_{2,3}=\rho_{0,3}^{exp.}\\ &p_{2,3}=0\\ &e_{2,3}=0 \end{aligned}\right\} \tag{15}$$

Inserting experimental results and imposing that $p_{2,1}=p_{2,2}$ and $v_{2,1}=v_{2,2}$ at the material interface renders a system that is analytically solvable. However, an approximative graphic solution is shown in Fig. 2. The equation of state for specimen one is reflected in a plane perpendicular to the v-axis at $v_{2,1}=1500\,m/s$ and the specimen two shock impedance curve $p=\rho_{0,2}^{exp.}u_{2,2}^{exp.}v$ intersects this curve at $v_{2,2}=1000\,m/s$.

Phase 3

When the shock wave front reaches the interface between specimens two and three the shock wave is reflected to specimen two and refracted into specimen three according to

$$\left.\begin{aligned} &\rho_{3,1}=\rho_{2,1}\\ &p_{3,1}=p_{2,1}\\ &e_{3,1}=e_{2,1} \end{aligned}\right\} \tag{16}$$

$$\left.\begin{array}{l}\rho_{3,2}\left(u_{3,2}-v_{3,2}\right)=\rho_{2,2}\left(u_{3,2}-v_{2,2}\right)\\ p_{3,2}-p_{2,2}=\rho_{2,2}\left(u_{3,2}-v_{2,2}\right)\left(v_{3,2}-v_{2,2}\right)\\ e_{3,2}-e_{2,2}=\frac{1}{2}\left(p_{3,2}+p_{2,2}\right)\left(\frac{1}{\rho_{2,2}}-\frac{1}{\rho_{3,2}}\right)\\ p_{3,2}=p_{2,2}+\frac{1}{2}\left(\rho_{2,2}+\rho_{3,2}\right)g_2\left(e_{3,2}-e_{2,2}\right)\end{array}\right\} \tag{17}$$

$$\left.\begin{array}{l}\rho_{3,3}\left(u_{3,3}-v_{3,3}\right)=\rho_{2,3}u_{3,3}\\ p_{3,3}=\rho_{2,3}u_{3,3}v_{3,3}\\ e_{3,3}=\frac{1}{2}p_{3,3}\left(\frac{1}{\rho_{2,3}}-\frac{1}{\rho_{3,3}}\right)\\ u_{3,3}=c_3+s_3v_{3,3}\end{array}\right\} \tag{18}$$

Imposing once again the conditions of equilibrium $p_{3,2}=p_{3,3}$ and continuity $v_{3,2}=v_{3,3}$ yields a system of equations from which the unknown variables are solved for. In specimen three we have

$$\left.\begin{array}{l}v_{3,3}=\frac{u_{3,3}^{exp.}-c_3}{s_3}\\ \rho_{3,3}=\frac{\rho_{2,3}}{1-\frac{1}{s_3}+\frac{c_3}{s_3u_{3,3}^{exp.}}}\\ p_{3,3}=\frac{\rho_{2,3}}{s_3}\left(u_{3,3}^{exp.}-c_3\right)u_{3,3}^{exp.}\\ e_{3,3}=\frac{\left(u_{3,3}^{exp.}-c_3\right)^2}{2s_3^2}\end{array}\right\} \tag{19}$$

2.2.2 Grout specimens

The thinner the disc the less the error due to the idealization that the shock wave passes through the disc at a constant velocity. But, for grout the minimum thickness is set by the aggregate size and was here chosen to be $10\,mm$.

The plane wave experiments were performed at FOI Grindsjön research centre during the period June to August 2002. The concrete grout discs with $\rho_0 = 2230\,kg/m^3$ were sawed out of a cylinder and then polished. Radial cracks appeared in some of the discs that were kept in air and to minimize the risc of fracture new discs were manufactured and kept in water until 3-18 hours before performing the experiments.

2.2.3 Plane wave generator

The plane wave generators used were designed and manufactured at FOI Grindsjön Research Centre. The device generates a circular plane wave with a diameter of $60\,mm$ at a pressure of $28\,GPa$. A disc of TNT was added as a first stage of damping to approximately $21\,GPa$.

2.2.4 Diagnostic tools

Two types of diagnostic tools were used, uniaxial piezoelectric stress gauges (PVDF) and piezoelectric pins. The output from the PVDF-gauges was converted by an integrator into a voltage signal that had been calibrated with respect to the applied stress. With the piezoelectric pins the time of arrival was registered at three points and this was used as a control of the quality of the shock wave. See Figure 3 for the positioning of the gauges and pins. The quality of the shock wave is here defined in terms of planarity as Q_p and symmetry as Q_s:

$$Q_p = \frac{2t^{centre}_{arrival}}{t^{side1}_{arrival} + t^{side2}_{arrival}} \quad (20)$$

$$Q_s = \frac{min(\Delta t^{side1}_{arrival}, \Delta t^{side2}_{arrival})}{max(\Delta t^{side1}_{arrival}, \Delta t^{side2}_{arrival})} \quad (21)$$

and from these a weight function w, indicating the significance of the measured shock wave velocity, is computed according to:

$$w = Q_p Q_s \quad (22)$$

Thus a plane wave with high quality approaches 1 and if the quality is poor it is lower.

The registrations were made using a LeCroy 9384M oscilloscope at a sampling frequence of $1\,GHz$. Photos of the gauges are found in Appendix C.

2.2.5 Set-up

The experimental set-up is shown in Figure 3 and in Appendix C. Note that in Figure 3 there are three discs of Lexan, while in the experiments this number varied from 1 to 4 discs. Vaseline was used between the discs to eliminate the gap due to the thickness of the PVDF-gauges.

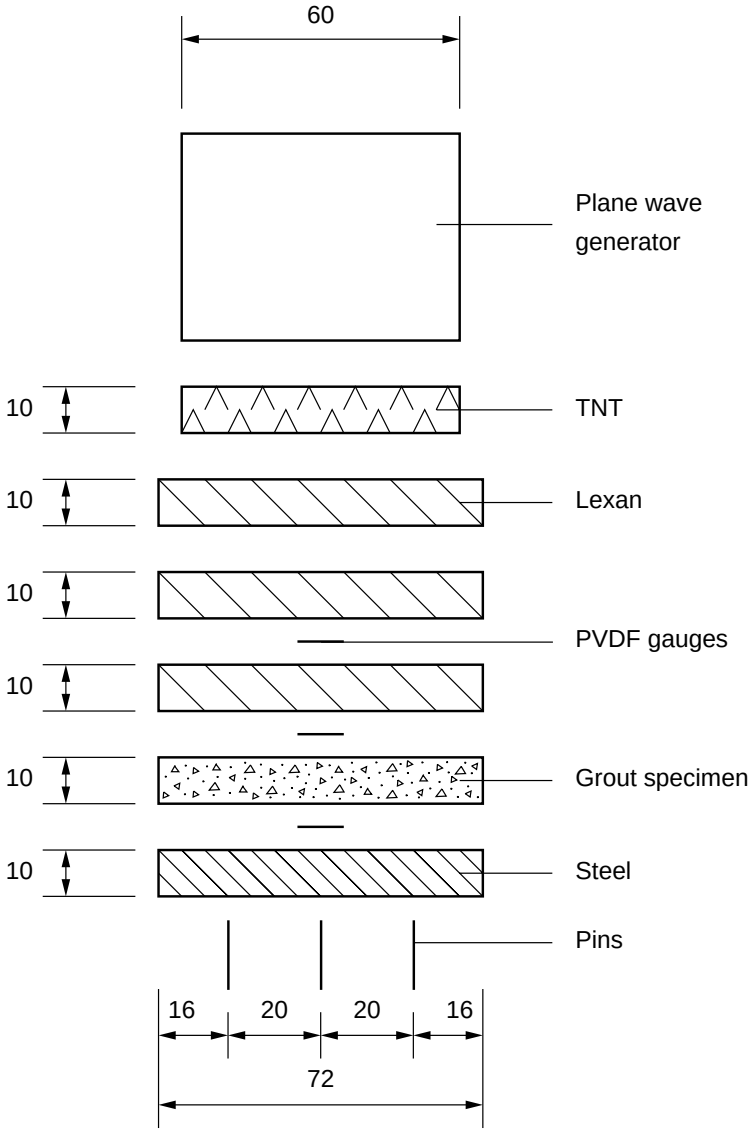

Figure 3. Sketch of the experimental set-up with the parts separated in the vertical direction for clarity. The total number of Lexan discs varied in the experiments.

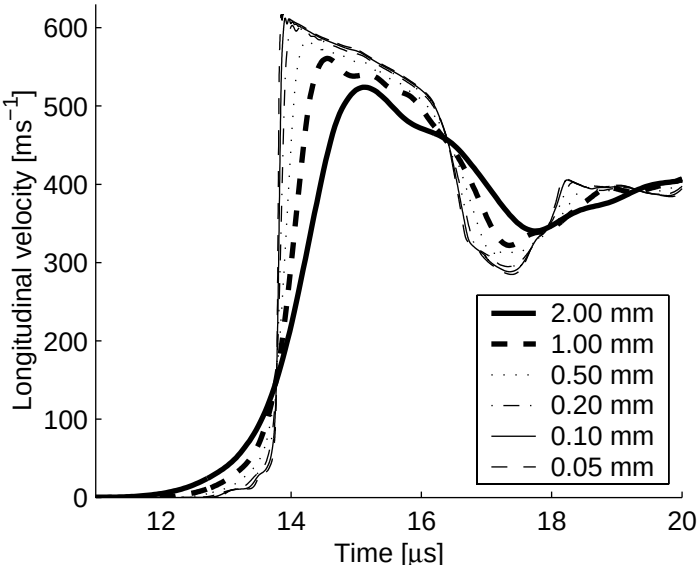

Figure 4. Velocity history for different finite element sizes

3 Results

3.1 Numerical analysis

3.1.1 Model convergence analysis

A one-dimensional, plane strain model was set up to perform a convergence analysis. The model consisted of $20\,mm$ TNT, $30\,mm$ Lexan, $10\,mm$ grout and $10\,mm$ steel. Different element sizes, varying from 0.05 to $2.00\,mm$, were used and the velocity history of a material point at the steel back-face was registered. The registrations are shown in Figure 4. It was concluded that an element size of $0.10\,mm$ resulted in a sufficiently accurate numerical solution.

3.1.2 Shock wave planarity analysis

The detonation pressure in the TNT of $21\,GPa$ was to be damped as much as possible without discrimination of the plane-strain state in the specimen. A two-dimensional model with rotational symmetry was set-up with $20\,mm$ TNT and $100\,mm$ Lexan. An analysis was carried out and registrations were made of the time of arrival and longitudinal stress for the shock wave. The results are shown in Figures 5 and 6. In the figures $x = 0\,mm$ represents the interface between explosive and damping material. The pressures and stresses are normalized with respect to the magnitude of the refracted stress. It was concluded that a maximum of $40\,mm$ Lexan could be used to maintain a plane strain state over the active area of the gauge.

3.1.3 Pressure levels in specimen

The resulting pressure loading of the grout specimen at different levels of damping, i.e. different Lexan thickness, is shown in Figure 7.

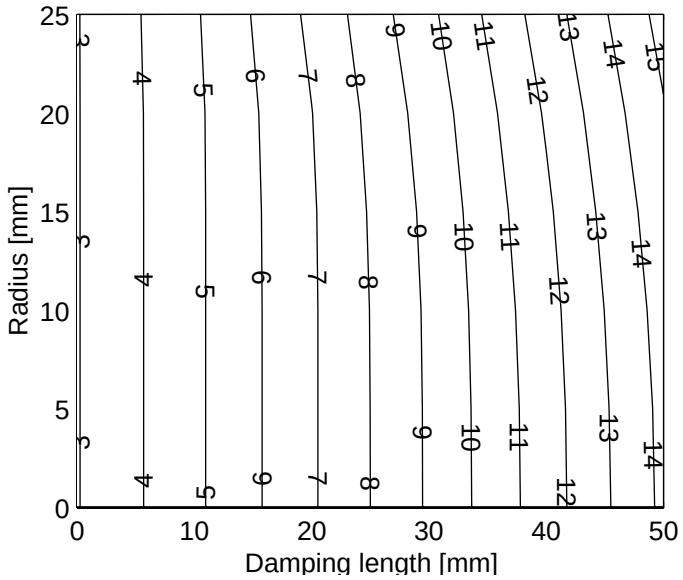

Figure 5. Iso-curves for shock wave arrival time [μs]

Table 2. Shock wave velocities and quality

Exp. no.	h	$u_{i,j}^{exp.}\,[m/s]$			Wave quality		
	$[mm]$	Lexan	Grout	Steel	Q_p	Q_s	w
1	38.48	No detonation					
2	19.25	5752	4663	5921	0.975	0.580	0.566
3	38.21	4429	4052	5863	0.977	0.856	0.836
4	19.11	x	x	x	0.974	0.705	0.687
5	19.12	5766	4835	5764	0.978	0.781	0.764
6	28.69	5156	4127	5884	0.980	0.998	0.978
7	28.68	5156	4346	6155	0.982	0.785	0.771
8	9.56	x	5345	5861	0.992	0.943	0.935
9	9.56	x	5311	5136	0.998	-1.484	-1.481
10	38.28	x	x	x	0.971	0.858	0.833

3.2 Plane wave experiments

The main results from the experiments are presented in Table 2 where h is the total damping length, ie. the Lexan thickness, and 'x' denotes failure of registration. All signals from the PVDF-gauges showed too low pressures why these are not used in the evaluation (see Chapter 4 for comments on this). The data from test number nine was rejected due to the poor wave quality and the results from the calculations of the Grüneisen constant g_2 are not given since the results were of an unsatisfying quality. Adjustments have been made of the times of arrival for the time of passage through the gauges and differences in cable length with 20 and 5 ns respectively (see also Appendix B). The experimental data were evaluated using the mathematical softwares Maple (version 7.0) and Matlab (version 6.5) and the derived results on primary shock wave velocities, particle velocities, pressure and densities are shown in Figures 8, 9, 10 and 11. In Table 3 and Figure 12 to 13 the results for the grout are presented.

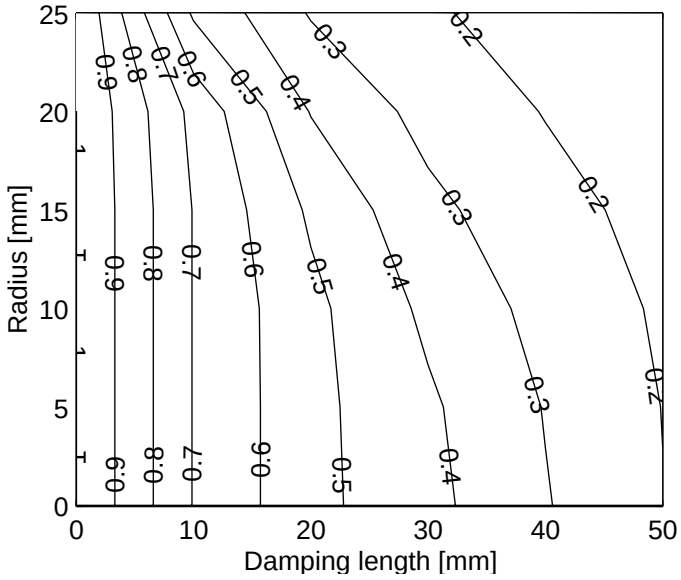

Figure 6. Iso-curves for normalized longitudinal stress

Table 3. Compiled results for grout

Test no.	$u_{2,2}^{exp.}\,[m/s]$	$v_{2,2}\,[m/s]$	$\rho_{2,2}\,[kg/m^3]$	$p_{2,2}\,[GPa]$	$e_{2,2}\,[kJ/kg]$
2	5752	1677	3482	17.4	1405
3	4429	910	2876	8.2	414
5	5766	1646	3381	17.7	1355
6	5156	1379	3350	12.7	951
7	5156	1331	3215	12.9	886

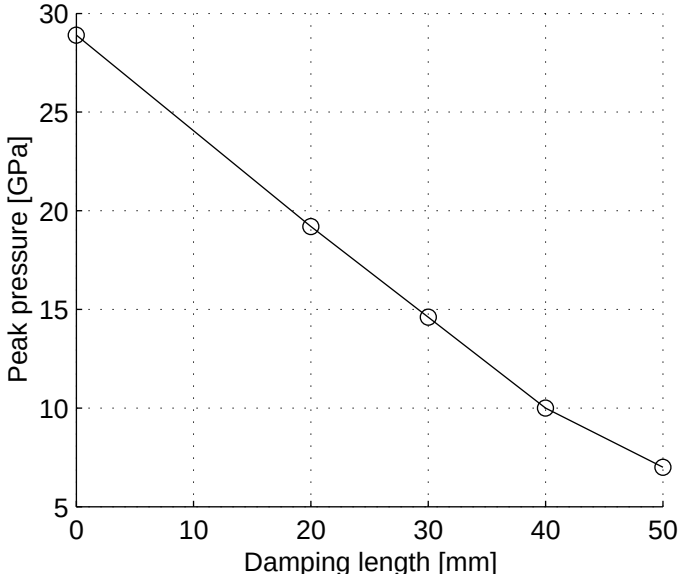

Figure 7. Calculated pressure loading at specimen front face

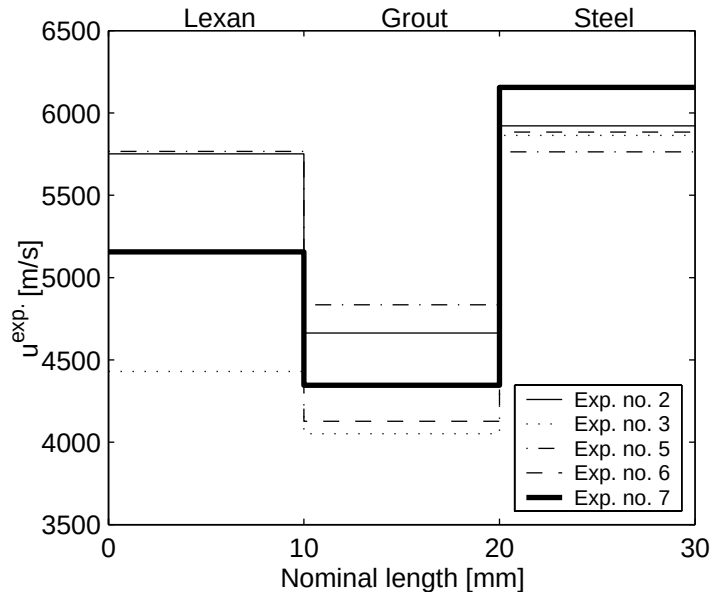

Figure 8. Primary shock wave velocities

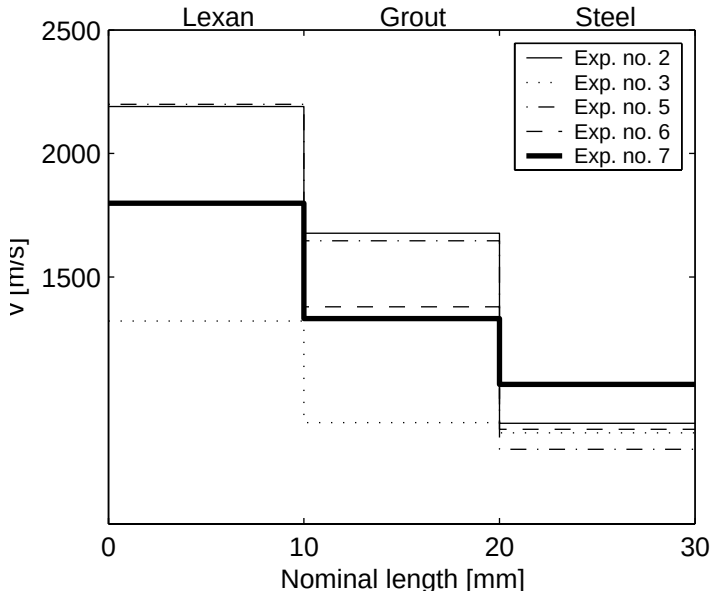

Figure 9. Primary particle velocities

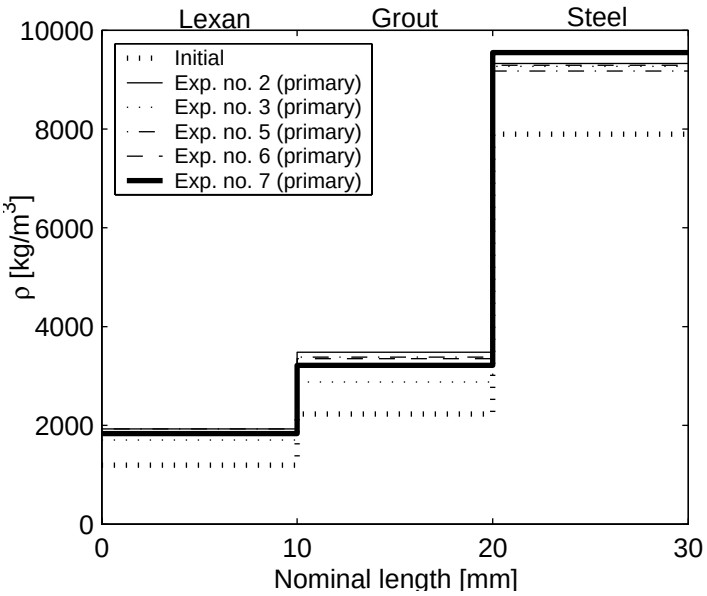

Figure 10. Initial and primary densities

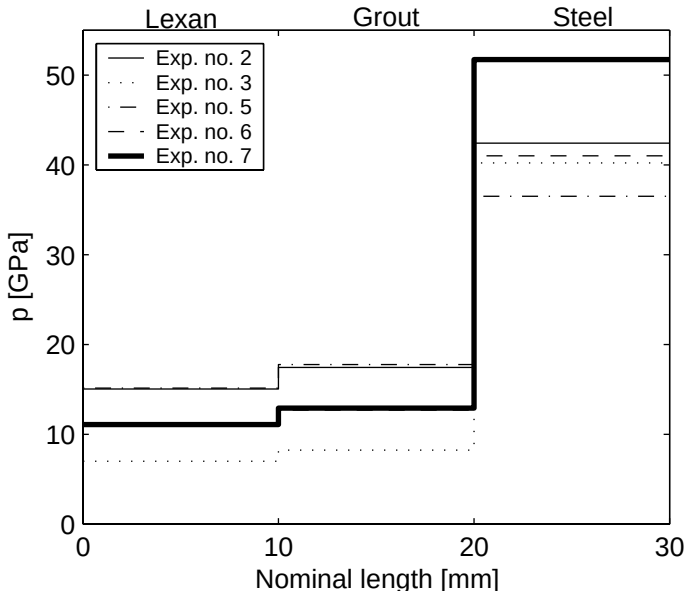

Figure 11. Primary pressures

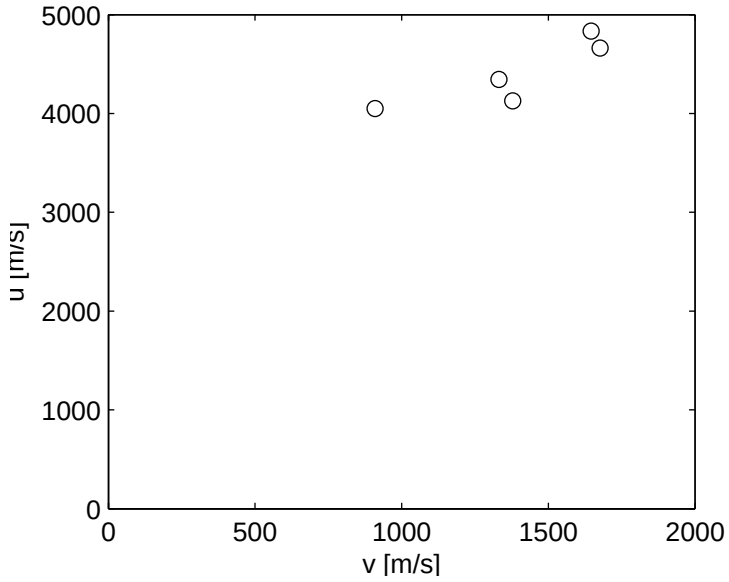

Figure 12. Results in $u - v$-space for the grout

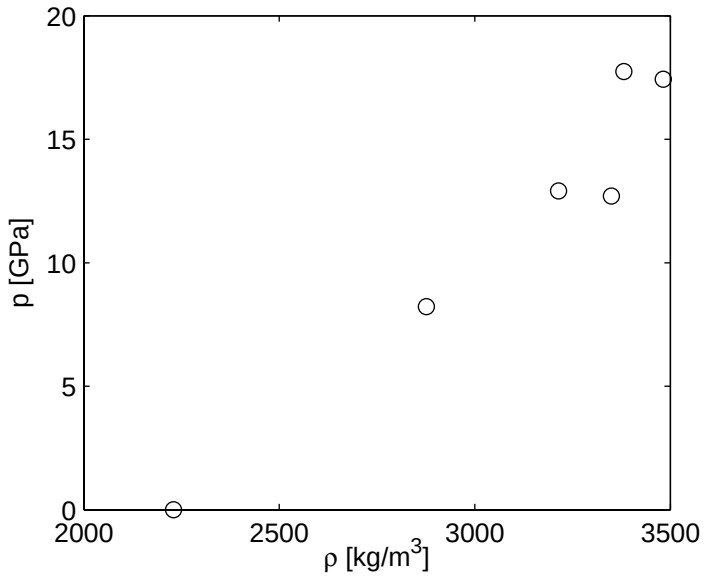

Figure 13. Results in $p - \rho$ -space for the grout

4 Discussion

A series of experiments on concrete grout loaded with plane shock waves have been conducted. This was done in order to evaluate the chosen method where the shock wave is generated by an explosively driven plane wave generator. Numerical simulations were performed to serve as a basis for the design of the experimental set-up.

The experimental results on the primary shock behaviour of the grout show good agreement with the numerical simulations. However, the amplitudes from the piezoelectric stress gauges were too low. The manufacturer of the gauges explains this with a short circuit in the gauges due to unprotected connections of the wires to the gauge tabs. The short circuit was probably due to a surge of high voltage or ionized gases produced by the tests. This short circuit can be avoided by a hermetical sealing of the connections with epoxy and by using small coaxial cables all the way to the gauge tabs.

The method to transmit an explosively generated plane shock wave to two specimens in contact with each other with known and unknown equations of state respectively has been used since the 1950's. The major drawback of this method is the difficulties to vary the transmitted pressure. Different types of high explosives, damping materials and confinements can be used to lower the magnitude of the pressure transmitted to a specimen, but the pressure levels are still much higher than those encountered in events with conventional projectiles. However, material characterization at these high pressure levels can be necessary for problems involving shaped charges.

Another method to investigate the volumetric behaviour of materials is the gun-propelled plate-impact method. The exit velocity of the plate-projectile can be varied in a much wider range and thus, the pressure transmitted to the specimen. The diagnostic tools needed are not destructed in the test and can be re-used, while the gauges in the explosively driven method are destroyed.

The first conclusion from this work is that the used method is to be used preferably for determining the volumetric behaviour at pressures in the range above $15\,GPa$. The explosive used determines the upper limit of the range. With Composition B in direct contact with a grout specimen a pressure of approximately $35\,GPa$ can be transmitted. For problems of conventional projectile penetration a gun-propelled technique is preferable since it can be used to extract data on the volumetric behaviour in a lower pressure range.

Secondly, an investigation should be carried out to determine how the free pore water in the grout discs influenced the results and as a first step in such an investigation the water content of three grout discs were studied. Disc *A* was covered with vaseline at the circular top and bottom faces to simulate the situation in the experimental set-up. Disc *B* had a volume of $48.322\ ml$ and free boundary. The volume of disc *C* was $48.528\ ml$. The mass of discs *A* and *B* was monitored for 20 hours and the resulting mass loss ratio is shown in Figure 14. After this disc *B* was kept in vacuum at $100^{\circ}\mathrm{C}$ for 7 hours resulting in a mass loss ratio of 0.068, or a water volume ratio of 0.15. Disc *C* was kept at room temperature and atmospheric pressure for six months resulting in a mass loss ratio of 0.036 or a water volume ratio of 0.077.

Finally, it is not always necessary to use calibrated PVDF-gauges. In some cases is it sufficient to use non-calibrated, i.e. cheaper, gauges that monitor only

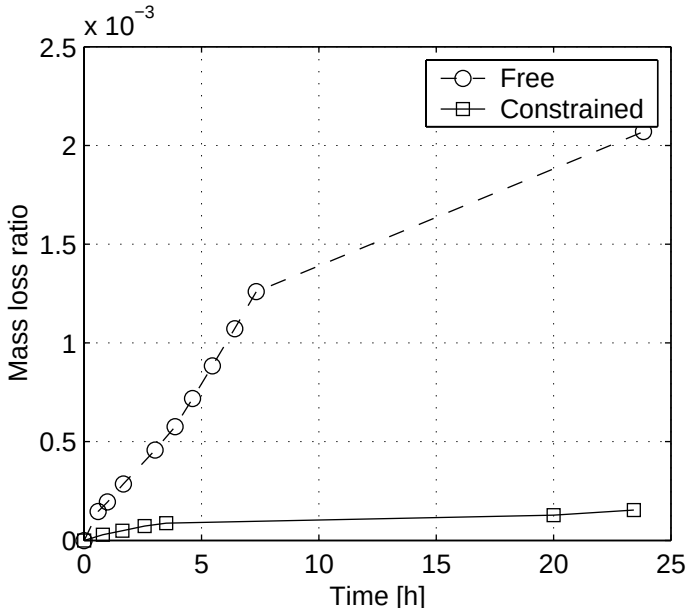

Figure 14. Measured mass loss ratio of grout discs

the time of arrival so that impedance matching with a material with known volumetric behaviour, such as Lexan or PMMA, can be performed. However, if calibrated gauges are used, for example if an elastic pre-cursor is anticipated, great care has to be taken in the preparations. The connections to the gauge tabs have to be hermetically sealed to avoid short circuits causing wrong registrations of the amplitudes.

References

[1] M. A. Meyers, *Dynamic behavior of materials*. Wiley-Interscience publication, New York (NY): Wiley, 1994.

[2] R. A. Graham, *Solids under high-pressure shock compression: mechanics, physics and chemistry*. High-pressure shock compression of condensed matter, New York (NY): Springer, 1993.

[3] C. A. Truesdell and R. A. Toupin, "The classical field theories," in *Encyclopedia of physics* (S. Flügge, ed.), vol. III/1, pp. 226–793, Berlin-Göttingen-Heidelberg: Springer-Verlag, 1960.

[4] Century Dynamics Incorporated, Horsham, *AUTODYN theory manual, revision 4.0*, 1998.

[5] C. A. Truesdell and W. Noll, "The non-linear field theories of mechanics," in *Encyclopedia of physics* (S. Flügge, ed.), vol. III/3, pp. 1–602, New York: Springer Verlag, 1965.

[6] E. L. Lee, H. C. Hornig, and J. W. Kury, "Adiabatic expansion of high explosive detonation products," Tech. Rep. UCRL-50422, University of California, Lawrence radiation laboratory, Livermore, CA, 1968.

[7] S. P. Marsh, ed., *LASL shock Hugoniot data*. Los Alamos series on dynamic material properties, Berkeley, CA: University of California press, 1980.

[8] W. Riedel, *Beton unter dynamischen Lasten: Meso- und makromechanische Modelle und ihre Parameter*. Doctoral thesis, Universität der Bundeswehr München, Freiburg, 2000.

[9] M. Wicklein and W. Riedel, "Mesomechanical characterization of a high strength concrete: Experimental investigations and material modelling," Tech. Rep. E 14/02, Ernst-Mach-Institute, EMI, Freiburg, apr 2002.

[10] S. Smeplass, "Høyfast betong til forsvarsformål-materialutvikling," tech. rep., Norges teknisk- naturvitenskapelige universitet, Trondheim, Norway, aug 1999. In norwegian.

[11] G. R. Johnson and W. H. Cook, "A constitutive model and data for metals subjected to large strains, high strain rates and high temperatures," pp. 541–547, 1983.

Appendix A

Constitutive material parameters

TNT

Reference density (g/cm3) : 1.63000E+00
Parameter A (kPa) : 3.73770E+08
Parameter B (kPa) : 3.74710E+06
Parameter R1 : 4.15000E+00
Parameter R2 : 9.00000E-01
Parameter W : 3.50000E-01
C-J Detonation velocity (m/s) : 6.93000E+03
C-J Energy / unit volume (kJ/m3) : 6.00000E+06
C-J Pressure (kPa) : 2.10000E+07

Grout

Porous density (g/cm3) : 2.23000E+00
Porous sound speed (m/s) : 2.96000E+03
Initial compaction pressure (kPa) : 4.50000E+04
Solid compaction pressure (kPa) : 1.40000E+07
Compaction exponent n : 3.00000E+00
Reference density (g/cm3) : 2.91000E+00
Gruneisen coefficient : 1.00600E+00
Parameter C1 (m/s) : 5.77400E+03
Parameter S1 : 1.00300E+00
Reference temperature (K) : 2.93000E+02
Specific heat (C.V.) (J/kgK) : 6.54000E+02
Shear modulus (kPa) : 1.66000E+07
Yield stress (kPa) : 1.35000E+05

Lexan

Reference density (g/cm3) : 1.19400E+00.
Gruneisen coefficient : 6.10000E-01
Parameter C1 (m/s) : 2.41800E+03
Parameter S1 : 1.52230E+00
Reference temperature (K) : 2.93000E+02
Specific heat (C.V.) (J/kgK) : 1.25600E+03
Shear modulus (kPa) : 2.10000E+06
Yield stress (kPa) : 6.00000E+04
Hydro tensile limit (PMIN) (kPa) : -9.00000E+08

Steel

Reference density (g/cm3) : 7.89600E+00
Gruneisen coefficient : 2.17000E+00

Parameter C1 (m/s) : 4.56900E+03
Parameter S1 : 1.49000E+00
Reference temperature (K) : 3.00000E+02
Specific heat (C.V.) (J/kgK) : 4.52000E+02
Shear modulus (kPa) : 8.18000E+07
Yield stress (kPa) : 3.50000E+05
Hardening constant (kPa) : 2.75000E+05
Hardening exponent : 3.60000E-01
Strain rate constant : 2.20000E-02
Thermal softening exponent : 1.00000E+00
Melting temperature (K) : 1.81100E+03

Appendix B

Registrations from diagnostic tools

Arrival times at the PVDF-gauges and the piezoelectric pins are taken at 1 V and 5 V respectively. Positions marked 'x' denotes failure to register signal.

Table 4. Extracted data from experiment no. 2

Material	$h\,[mm]$	$t_{arrival}\,[\mu s]$	$V_{peak}\,[V]$
Lexan	9.65	-	-
S-5096 G2 P2	0.08	13.588	4.131
Lexan	9.60	-	-
S-5096 G3 P2	0.08	15.277	6.425
Grout	10.51	-	-
S-5096 G2 P1	0.08	17.551	3.569
Steel	10.51	-	-
Pins	-	19.702, 19.341, 19.963	-

Table 5. Extracted data from experiment no. 3

Material	$h\,[mm]$	$t_{arrival}\,[\mu s]$	$V_{peak}\,[V]$
Lexan	28.66	-	-
S-5096 G3 P4	0.08	17.058	5.856
Lexan	9.55	-	-
S-5096 G1 P5	0.08	19.234	4.605
Grout	10.88	-	-
S-5096 G2 P4	0.08	21.939	6.730
Steel	10.05	-	-
Pins	-	24.260, 23.668, 24.175	-

Table 6. Extracted data from experiment no. 4

Material	$h\,[mm]$	$t_{arrival}\,[\mu s]$	$V_{peak}\,[V]$
Lexan	9.56	-	-
S-5096 G6 P8	0.08	x	x
Lexan	9.55	-	-
S-5096 G5 P4	0.08	x	x
Grout	10.88	-	-
S-5096 G5 P8	0.08	x	x
Steel	9.95	-	-
Pins	-	19.683, 19.262, 19.863	-

Table 7. Extracted data from experiment no. 5

Material	$h\,[mm]$	$t_{arrival}\,[\mu s]$	$V_{peak}\,[V]$
Lexan	9.56		
S-5096 G1 P9	0.08	13.512	3.312
Lexan	9.56		
S-5096 G5 P9	0.08	15.190	5.125
Grout	10.99	-	-
S-5096 G5 P7	0.08	17.483	2.000
Steel	9.81	-	-
Pins	-	19.694, 19.200, 19.586	-

Table 8. Extracted data from experiment no. 6

Material	$h\,[mm]$	$t_{arrival}\,[\mu s]$	$V_{peak}\,[V]$
Lexan	19.13	-	-
S-5096 G6 P9	0.08	15.248	5.312
Lexan	9.56	-	-
S-5096 G4 P9	0.08	17.122	5.156
Grout	10.02	-	-
S-5096 G2 P6	0.08	19.570	6.187
Steel	9.82	-	-
Pins	-	21.694, 21.254, 21.693	-

Table 9. Extracted data from experiment no. 7

Material	$h\,[mm]$	$t_{arrival}\,[\mu s]$	$V_{peak}\,[V]$
Lexan	19.12	-	-
S-5096 G3 P6	0.08	15.229	5.625
Lexan	9.56	-	-
S-5096 G3 P9	0.08	17.103	6.969
Grout	10.97	-	-
S-5096 G3 P7	0.08	19.647	0.562
Steel	9.94	-	-
Pins	-	21.620, 21.277, 21.714	-

Table 10. Extracted data from experiment no. 8

Material	$h\,[mm]$	$t_{arrival}\,[\mu s]$	$V_{peak}\,[V]$
S-5096 G2 P9	0.08	x	0.812
Lexan	9.56	-	-
S-5096 G4 P7	0.08	13.480	4.688
Grout	10.77	-	-
S-5096 G3 P8	0.08	15.515	3.687
Steel	10.07	-	-
Pins	-	17.381, 17.248, 17.389	-

Table 11. Extracted data from experiment no. 9

Material	$h\,[mm]$	$t_{arrival}\,[\mu s]$	$V_{peak}\,[V]$
S-5096 G4 P5	0.08	x	1.125
Lexan	9.56	-	-
S-5096 G6 P6	0.08	13.660	3.625
Grout	10.93	-	-
S-5096 G6 P7	0.08	15.738	4.125
Steel	10.03	-	-
Pins	-	17.549, 17.706, 17.939	-

Table 12. Extracted data from experiment no. 10

Material	$h\,[mm]$	$t_{arrival}\,[\mu s]$	$V_{peak}\,[V]$
Lexan	28.72	-	-
S-5096 G5 P6	0.08	x	x
Lexan	9.56	-	-
S-5096 G1 P6	0.08	x	x
Grout		-	-
S-5096 G2 P8	0.08	x	x
Steel		-	-
Pins	-	24.363, 23.595, 24.254	-

Appendix C

Photos

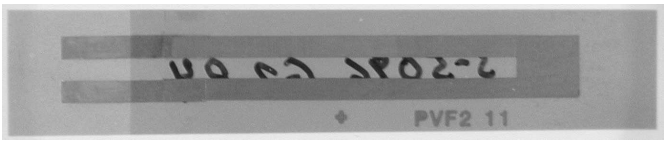

Figure 15. PVDF-gauge (active area $6.35 \times 6.35 \times 0.08\,mm$)

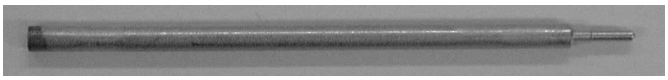

Figure 16. Piezoelectric pin (length $56\,mm$, diameter $2.36\,mm$)

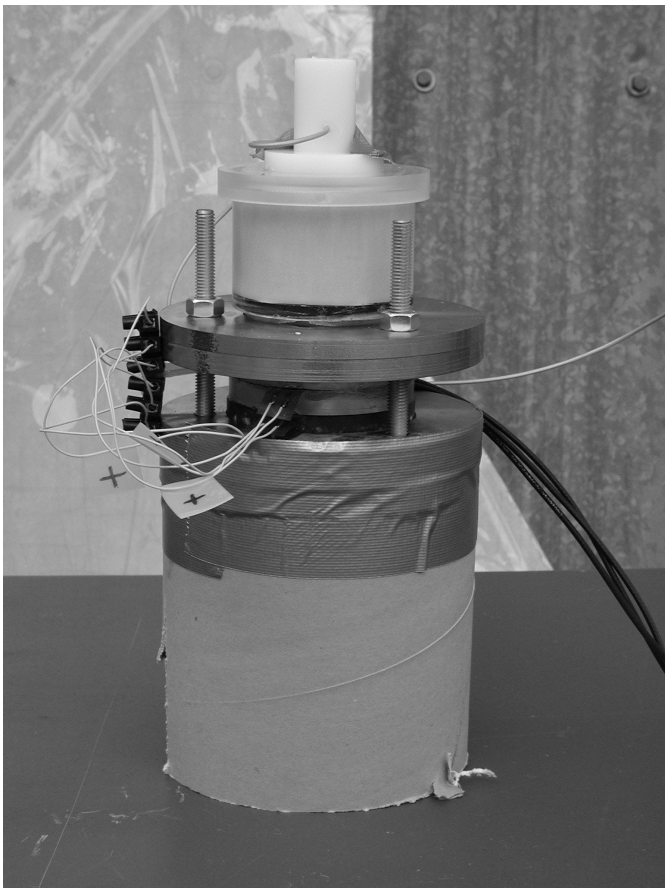

Figure 17. Experimental set-up

Issuing organisation
FOI – Swedish Defence Research Agency
Weapons and protection division
SE-147 25 TUMBA

Report number, ISRN
FOI-R–0550–SE

Report type
Methodology report

Month year
December 2002

Project number
E2011

Customers code
5. Commissioned research

Research area code
5. Combat

Sub area code
53. Protection and fortification

Author(s)
Mattias Unosson

Project manager
Johan Magnusson

Approved by
Michael Jacob
Head of department

Scientifically and technically responsible
Henrik Almström
Research director

Report title
Shock wave loading of concrete grout using a plane wave generator

Abstract
In the report a series of experiments is presented where solid discs of concrete grout are loaded with plane shock waves. Plane wave generators with high explosives were used for the loading, and registration of stress and times of arrival were made using calibrated piezoelectric stress gauges (PVDF) and piezoelectric pins. Finite element analysis was used to design the experimental set-up. From the experimental results, points on the equation of state for the grout were derived through impedance matching with Lexan. The amplitudes from the gauges, representing the pressure level, were too low due to shortage of the gauges. The grout specimens had been kept in water prior to the experiments to minimize the risk of cracks. The conclusions were that the experimental technique used is suitable for deriving points on the equation of state at pressure levels above $15\,GPa$.

Keywords
shock wave;equation of state;concrete grout;simulation;plane wave experiments

Further bibliographic information

ISSN
ISSN 1650-1942

Pages
39

Language
English

Price
According to price list

Security classification
Unclassified

Utgivare	Rapportnummer, ISRN	Klassificering
Totalförsvarets Forskningsinstitut – FOI Avdelningen för vapen och skydd 147 25 TUMBA	FOI-R–0550–SE	Metodrapport
	Månad år December 2002	Projektnummer E2011
	Verksamhetsgren 5. Uppdragsfinansierad verksamhet	
	Forskningsområde 5. Bekämpning	
	Delområde 53. Skydd och anläggningsteknik	

Författare	Projektledare
Mattias Unosson	Johan Magnusson
	Godkänd av Michael Jacob Chef, Institutionen för skydd och material
	Tekniskt och/eller vetenskapligt ansvarig Henrik Almström Forskningschef

Rapporttitel

Stötvågsbelastning av betongpasta med en planvågsgenererande laddning

Sammanfattning

I rapporten presenteras en serie experiment i vilken cirkulära skivor av betongpasta belastas med plana stötvågor. Planvågsgenererande laddningar användes för att skapa belastningen och registrering av spänning och ankomsttid gjordes med kalibrerade piezoelektriska spänningsgivare (PVDF) och piezoelektriska pinnar. Finita elementanalyser användes för design av försöksuppställningen. Från de experimentella resultaten togs punkter på tillståndsekvationen fram genom impedansanpassning med Lexan. De registrerade amplituderna från PVDF-givarna var för låga pågrund av kortslutning under stötvågens passage. Skivorna av betongpasta förvarades i vatten fram till försökens genomförande för att minimera risken för sprickor. Slutsatserna var att provningmetoden är lämplig för att ta fram punkteröver $15\,GPa$ påtillståndsekvationen.

Nyckelord

stötvåg;tillståndsekvation;betongpasta;simulering;planvågsexperiment

Övriga bibliografiska uppgifter

ISSN	Antal sidor	Språk
ISSN 1650-1942	39	Engelska
Distribution enligt missiv -	Pris Enligt prislista	
	Sekretess Öppen	